inorganic compounds

Lithiotantite, ideally LiTa$_3$O$_8$

Luiz A.D. Menezes Filho,[a] Hexiong Yang,[b]* Robert T. Downs,[b] Mário L. S. C. Chaves[a] and Aba C. Persiano[c]

[a]Instituto de Geociências, Universidade Federal de Minas Gerais, Av. Antônio Carlos, 6627,31270-901, Belo Horizonte, MG, Brazil, [b]Department of Geosciences, University of Arizona, 1040 E. 4th Street, Tucson, Arizona 85721-0077, USA, and [c]Departamento de Fisica, Universidade Federal de Minas Gerais, CP 702, 30123-970, Belo Horizonte, MG, Brazil
Correspondence e-mail: hyang@u.arizona.edu

Lithiotantite (lithium tritantalum octaoxide) and lithiowodginite are natural dimorphs of LiTa$_3$O$_8$, corresponding to the laboratory-synthesized *L*-LiTa$_3$O$_8$ (low-temperature form) and *M*-LiTa$_3$O$_8$ (intermediate-temperature form) phases, respectively. Based on single-crystal X-ray diffraction data, this study presents the first structure determination of lithiotantite from a new locality, the Murundu mine, Jenipapo District, Itinga, Minas Gerais, Brazil. Lithiotantite is isotypic with LiNb$_3$O$_8$ and its structure is composed of a slightly distorted hexagonal close-packed array of O atoms stacked in the [$\bar{1}$01] direction, with the metal atoms occupying half of the octahedral sites. There are four symmetrically non-equivalent cation sites, with three of them occupied mainly by (Ta^{5+} + Nb^{5+}) and one by Li$^+$. The four distinct octahedra share edges, forming two types of zigzag chains (*A* and *B*) extending along the *b* axis. The *A* chains are built exclusively of (Ta,Nb)O$_6$ octahedra (*M*1 and *M*2), whereas the *B* chains consist of alternating (Ta,Nb)O$_6$ and LiO$_6$ octahedra (*M*3 and *M*4, respectively). The average *M*1—O, *M*2—O, *M*3—O and *M*4—O bond lengths are 2.011, 2.004, 1.984, and 2.188 Å, respectively. Among the four octahedra, *M*3 is the least distorted and *M*4 the most. The refined Ta contents at the *M*1, *M*2 and *M*3 sites are 0.641 (2), 0.665 (2), and 0.874 (2), respectively, indicating a strong preference of Ta^{5+} for *M*3 in the *B* chain. The refined composition of the crystal investigated is Li$_{0.96}$Mn$_{0.03}$Na$_{0.01}$Nb$_{0.82}$Ta$_{2.18}$O$_8$.

Related literature

For lithiotantite and isostructural materials, see: Voloshin *et al.* (1983); Lundberg (1971); Gatehouse & Leverett (1972). For lithiowodginite and wodginite-type materials, see: Voloshin *et al.* (1990); Ferguson *et al.* (1976); Gatehouse *et al.* (1976); Santoro *et al.* (1977); Erict *et al.* (1992). For structural and phase-stability information on the LiTa$_3$O$_8$ system, see: Nord & Thomas (1978); Fallon *et al.* (1979); Hodeau *et al.* (1983, 1984); Allemann *et al.* (1996). For properties and applications of LiTa$_3$O$_8$ and LiNb$_3$O$_8$, see: Subasri & Sreedharan (1997); Akazawa & Shimada (2007); Zhang *et al.* (2008); Muller *et al.* (2011). For the definition of polyhedral distortion, see: Robinson *et al.* (1971).

Experimental

Crystal data

Li$_{0.96}$Mn$_{0.03}$Na$_{0.01}$Nb$_{0.82}$Ta$_{2.18}$O$_8$	V = 546.75 (5) Å^3
M_r = 607.20	Z = 4
Monoclinic, $P2_1/c$	Mo $K\alpha$ radiation
a = 7.4425 (4) Å	μ = 45.28 mm^{-1}
b = 5.0493 (3) Å	T = 293 K
c = 15.2452 (7) Å	0.06 × 0.05 × 0.05 mm
β = 107.381 (3)°	

Data collection

Bruker APEXII CCD area-detector diffractometer	8136 measured reflections
	1983 independent reflections
Absorption correction: multi-scan (*SADABS*; Sheldrick, 2005)	1683 reflections with I > 2σ(I)
T_{min} = 0.172, T_{max} = 0.211	R_{int} = 0.027

Refinement

R[F^2 > 2σ(F^2)] = 0.028	71 parameters
wR(F^2) = 0.058	1 restraint
S = 1.35	$\Delta\rho_{max}$ = 2.02 e Å^{-3}
1983 reflections	$\Delta\rho_{min}$ = −1.92 e Å^{-3}

Data collection: *APEX2* (Bruker, 2004); cell refinement: *SAINT* (Bruker, 2004); data reduction: *SAINT*; program(s) used to solve structure: *SHELXS97* (Sheldrick, 2008); program(s) used to refine structure: *SHELXL97* (Sheldrick, 2008); molecular graphics: *Xtal-Draw* (Downs & Hall-Wallace, 2003); software used to prepare material for publication: *publCIF* (Westrip, 2010).

Supplementary data and figures for this paper are available from the IUCr electronic archives (Reference: BR2193).

References

Akazawa, H. & Shimada, M. (2007). *J. Mater. Res.* **22**, 1726–1736.
Allemann, J. A., Xia, Y., Morriss, A. P., Wilkinson, A. P., Eckert, E., Speck, J. S., Levi, C. G. & Lange, F. F. (1996). *J. Mater. Res.* **11**, 2376–2387.
Bruker (2004). *APEX2* and *SAINT*. Bruker AXS Inc., Madison, Wisconsin, USA.
Downs, R. T. & Hall-Wallace, M. (2003). *Am. Mineral.* **88**, 247–250.
Erict, T. S., Hawthorne, F. C. & Černý, P. (1992). *Can. Mineral.* **30**, 597–611.
Fallon, G. D., Gatehouse, B. M., Roth, R. S. & Roth, S. A. (1979). *J. Solid State Chem.* **27**, 255–259.
Ferguson, R. B., Hawthorne, F. C. & Grice, J. D. (1976). *Can. Mineral.* **14**, 550–560.
Gatehouse, B. M. & Leverett, P. (1972). *Cryst. Struct. Commun.* **1**, 83–86.
Gatehouse, B. M., Negas, T. & Roth, R. S. (1976). *J. Solid State Chem.* **18**, 1–7.
Hodeau, J. L., Marezio, M., Santoro, A. & Roth, R. S. (1983). *Solid State Ionics*, **9&10**, 78-82.
Hodeau, J. L., Marezio, M., Santoro, A. & Roth, R. S. (1984). *J. Solid State Chem.* **51**, 275–292.
Lundberg, M. (1971). *Acta Chem. Scand.* **25**, 3337–3346.

inorganic compounds

Muller, H. G., Stapleton, A. D., Foran, B. J., Radhakrishnan, G., Kim, H. I., Adams, P. M., Lipeles, R. A. & Herman, P. (2011). *J. Appl. Phys.* **110**, 033539 (1–7).

Nord, A. G. & Thomas, J. O. (1978). *Acta Chem. Scand. Ser. A*, **32**, 539–544.

Robinson, K., Gibbs, G. V. & Ribbe, P. H. (1971). *Science*, **172**, 567–570.

Santoro, A., Roth, R. S. & Minor, D. (1977). *Acta Cryst.* B**33**, 3945–3947.

Sheldrick, G. M. (2005). *SADABS*. University of Göttingen, Germany.

Sheldrick, G. M. (2008). *Acta Cryst.* A**64**, 112–122.

Subasri, R. & Sreedharan, O. M. (1997). *Mater. Lett.* **30**, 289–292.

Voloshin, A. V., Pakhomovskii, Y. A. & Bakhchisaraitsev, A. Y. (1990). *Mineral. Zh.*, **12**, 94–100.

Voloshin, A. V., Pakhomovskii, Y. A., Stepanov, V. I. & Tyusheva, F. N. (1983). *Mineral. Zh.* **5**, 91–95.

Westrip, S. P. (2010). *J. Appl. Cryst.* **43**, 920–925.

Zhang, D., Huang, D., Li, J. & Li, K. (2008). *J. Inorg. Mater.* **23**, 1106–1110.

supporting information

Lithiotantite, ideally LiTa$_3$O$_8$

Luiz A.D. Menezes Filho, Hexiong Yang, Robert T. Downs, Mário L. S. C. Chaves and Aba C. Persiano

S1. Comment

The outstanding electro-optical properties of lithium tantalate, LiTa$_3$O$_8$, and lithium niobate, LiNb$_3$O$_8$, have made them leading functional materials for numerous applications, such as electro-optic modulators, surface acoustic wave devices, frequency-doubled lasers, second-harmonic generators, beam deflectors, waveguides, and holographic data processing devices (*e.g.*, Subasri & Sreedharan, 1997; Akazawa & Shimada, 2007; Zhang *et al.*, 2008; Muller *et al.*, 2011). However, unlike LiNb$_3$O$_8$, which maintains the *P*2$_1$/*c* symmetry up to its incongruent melting point, LiTa$_3$O$_8$ is trimorphic, depending on its formation temperature (Allemann *et al.*, 1996). Below 1063 K, LiTa$_3$O$_8$ crystallizes in the *P*2$_1$/*c* symmetry (designated as *L*-LiTa$_3$O$_8$). Above 1063 K, *L*-LiTa$_3$O$_8$ transforms irreversibly to the intermediate-temperature *C*2/*c* form (*M*-LiTa$_3$O$_8$), which further transforms irreversibly to the high-temperature *Pmmn* structure (H-LiTa$_3$O$_8$) above 1393 K.

The crystal structure of *M*-LiTa$_3$O$_8$ was first determined by Gatehouse *et al.* (1976), who showed it to be monoclinic with space group *C*2/*c* and unit-cell parameters *a* =9.413 (5), *b* = 11.522 (6), *c* = 5.050 (3) Å, *β* = 91.1 (1)°. This phase is isotypic with the mineral wodginite, MnSnTa$_2$O$_8$ (Ferguson *et al.*, 1976; Erict *et al.*, 1992). A further refinement of the *M*-LiTa$_3$O$_8$ structure by Santoro *et al.* (1977) using neutron powder-diffraction data located the Li atom, which was not found in the X-ray diffraction study by Gatehouse *et al.* (1976). In contrast, the structure of H-LiTa$_3$O$_8$ has been investigated quite intensively, confirming its real symmetry to be *Pmmn* with unit-cell parameters *a* =16.718 (2), *b* = 7.696 (1), *c* = 8.931 (1) Å (Hodeau *et al.*, 1983, 1984), rather than *Pmma* with unit-cell parameters *a* =16.702 (8), *b* = 3.840 (4), *c* = 8.929 (5) Å (Nord & Thomas, 1978; Fallon *et al.*, 1979). Yet, no structure study has been reported for *L*-LiTa$_3$O$_8$ thus far. From rotation and Weissenberg photographic measurements, Gatehouse & Leverett (1972) obtained unit-cell parameters *a* = 7.41 (5), *b* = 5.10 (6), *c* = 15.12 (10) Å, *β* = 107.2 (1)°, and space group *P*2$_1$/*c* for *L*-LiTa$_3$O$_8$, suggesting that this phase is the Ta-analogue of LiNb$_3$O$_8$ (Lundberg, 1971). Interestingly, Voloshin *et al.* (1983) described a new mineral, lithiotantite, with the empirical chemical formula Li$_{0.92}$(Ta$_{1.90}$Nb$_{1.10}$Sn$_{0.02}$)$_{\Sigma=3.02}$O$_8$ or ideally LiTa$_3$O$_8$, from granite pegmatites in Eastern Kazakhstan. The new mineral possesses space group *P*2$_1$/*c* and unit-cell parameters *a* = 7.444, *b* = 5.044, *c* = 15.255 Å, *β* = 107.18°. Although all reported crystallographic data suggest that lithiotantite is actually *L*-LiTa$_3$O$_8$, it is unclear how Nb in the natural sample is distributed among three cation sites found in the isostructural LiNb$_3$O$_8$ (Lundberg, 1971). On the basis of single-crystal X-ray diffraction data, this study reports the first structure refinement of lithiotantite found from a new locality, the Jenipapo District, Itinga, Minas Gerais, Brazil.

Lithiotantite is isotypic with LiNb$_3$O$_8$ (Lundberg, 1971; Gatehouse & Leverett, 1972). Its structure consists of a slightly distorted hexagonal close-packed array of oxygen atoms stacked in the [-1 0 1] direction, with the metal atoms occupying half of the octahedral sites. There are four symmetrically nonequivalent cation sites, M1, M2, M3, and M4 (Fig. 1), with the first three occupied mainly by (Ta + Nb) and the last one by Li. The four distinct octahedra share edges to form two

types of zigzag chains (*A*- and *B*-chains) extending along the *b* axis (Fig. 2). The *A*-chains are built exclusively of (Ta,Nb)O_6 octahedra (M1 and M2), whereas the *B*-chains consist of alternating (Ta,Nb)O_6 and LiO_6 octahedra (M3 and M4, respectively). The refined Ta contents are 0.641 (2), 0.665 (2), and 0.874 (2) for M1, M2, and M3, respectively, indicating a relatively strong preference of Ta^{5+} on M3 over M1 or M2. The average M1—O, M2—O, M3—O, and M4—O bond distances are 2.011, 2.004, 1.984, and 2.188 Å, respectively. Among the four octahedra, M4 is the most distorted and M3 the least, as measured by the values of the octahedral angle variance (OAV) (Robinson *et al.*, 1971), which are 88, 81, 35, and 98° for the M1, M2, M3, and M4 octahedra, respectively. This observation is the direct consequence of the octahedral linkage within the two different chains. In the *B*-chain, the M4 octahedron occupied primarily by Li^+ is by far more weakly-bonded than M3 occupied by (Ta^{5+} + Nb^{5+}). Hence, for the two octahedra to share edges to form the chains, the relatively large M4 octahedron has to make more adjustments to fit to the configuration of the M3 octahedron and to minimize the cation-cation repulsion across the shared edges, thus resulting in its greater distortion. For the M1 and M2 octahedra that are occupied by the similar ratios of Ta/Nb, the cation-cation repulsion between the two across the shared edges is markedly stronger than that between M3 and M4. Therefore, the M1 and M2 octahedra exhibit similar OAV values and are more distorted than M3.

Gatehouse *et al.* (1976) demonstrated that *M*-$LiTa_3O_8$ is isomorphous with the mineral wodginite and presented a comprehensive structural comparison between *M*-$LiTa_3O_8$ and $LiNb_3O_8$. The mineral lithiowodginite, ideally $LiTa_3O_8$, a member of the wodginite group, was later described by Voloshin *et al.* (1990). With the discovery of lithiotantite (Voloshin *et al.*, 1983), isostructural with *L*-$LiTa_3O_8$ and $LiNb_3O_8$, one may postulate the possible existence of a natural $LiTa_3O_8$ phase with the H-$LiTa_3O_8$-type structure, as well as a natural Nb-analogue of lithiotantite.

S2. Experimental

The lithiotantite specimen used in this study is from the Murundu mine, the Jenipapo District, Itinga, Minas Gerais, Brazil and is in the collection of the RRUFF project (deposition No. R100165; http://rruff.info). Its chemical composition was analyzed with a Jeol JXA-8900 electron microprobe at the conditions of 20 kV and 25 nA. Counting times on peaks and backgrounds of the X-ray lines were 10 and 5 s, respectively. Raw data were corrected using the PRZ procedure, which gave (wt%) Ta_2O_5 = 78.5 (9), Nb_2O_5 = 17.1 (7), SnO_2 = 0.7 (3), MnO = 0.20 (10), FeO = 0.06 (3), Na_2O = 0.06 (3) (average of 9 analysis points). Li_2O was added to bring the total cation sums to 4.0 based on 8 O atoms, while maintaining the charge balance, yielding a chemical formula $(Li_{0.96}Na_{0.01}Mn^{2+}_{0.02}Fe^{2+}_{0.01})_{\sim\Sigma=1.00}(Ta_{2.18}Nb_{0.79}Sn_{0.03})_{\Sigma=3.00}O_8$.

S3. Refinement

For simplicity, during the structure refinement, the trace amount of Fe was treated as Mn, and Sn (0.03 apfu) as Nb, giving rise to a structural formula $(Li_{0.96}Na_{0.01}Mn^{2+}_{0.03})_{\Sigma=1.00}(Ta_{2.18}Nb_{0.83})_{\Sigma=3.00}O_8$, which was used throughout the structure refinements. Because a preliminary refinement showed that anisotropic displacement parameters were non-positive defined for M4 (mainly Li) and two O atoms, due most likely to the obvious inhomogeneity of the studied samples (Fig. 3), M4 and all O atoms were refined with isotropic displacement parameters only. In Figure 3, the contrast in darkness reflects the relative distribution of Ta vs. Nb in the sample. The distributions of Ta and Nb among the three octahedral sites were refined with their total amounts constrained to the above simplified formula. The final refinement indicates relatively large GOF value. We attempted to refine the Li position with a split-site model (or disordered model). Although the final *R* factor was slightly reduced from 0.0273 to 0.0271, the GOF value is essentially unchanged (still above 1.3). We tried to omit six bad reflections with Fo^2-Fc^2 > 7.0, but still failed to improve the GOF value. Even with the model of the split Li positions, the anisotropic displacement for Li is still non-positive definite. Thus, we believe that all of these

may result from the obvious inhomogeneities of our natural sample. In the past, we have noticed that a structure refinement may give rise to a large GOF value when the sample is not homogenous (like our current case, or with fine exsolutions, or badly twinned). In addition, we also tried to allow all oxygen atoms to be refined with anisotropic displacements. Yet, that only reduced the R factor to 0.0268 and the Li atom is still non-positive definite. The highest residual peak in the difference Fourier maps was located at (0.4240, 0.2970, 0.2913), 0.78 Å from M3, and the deepest hole at (0.0221, 0.1663, 0.3115), 0.64 Å from M2.
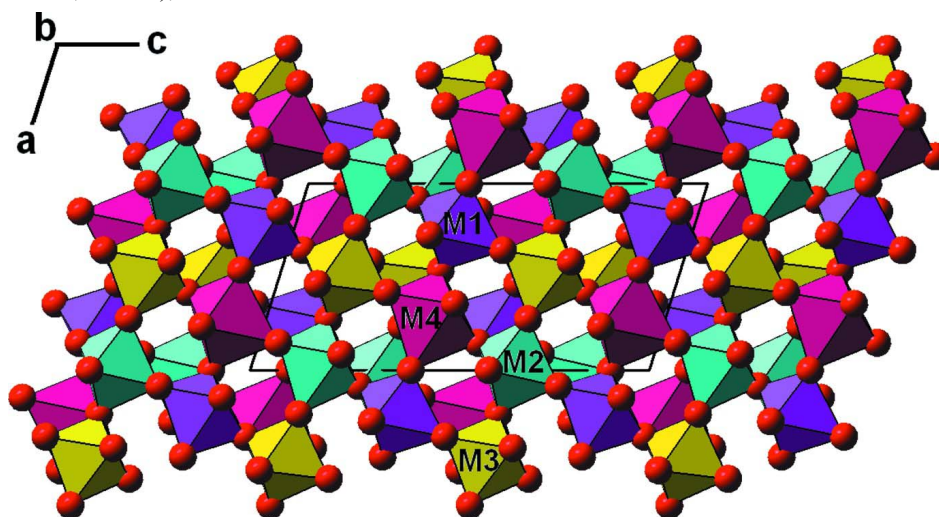
Figure 1

Crystal structure of lithiotantite viewed along [010]. Red spheres represent oxygen atoms. The purple, pale blue, yellow, and red octahedra represent M1, M2, M3, and M4 octahedra, respectively.
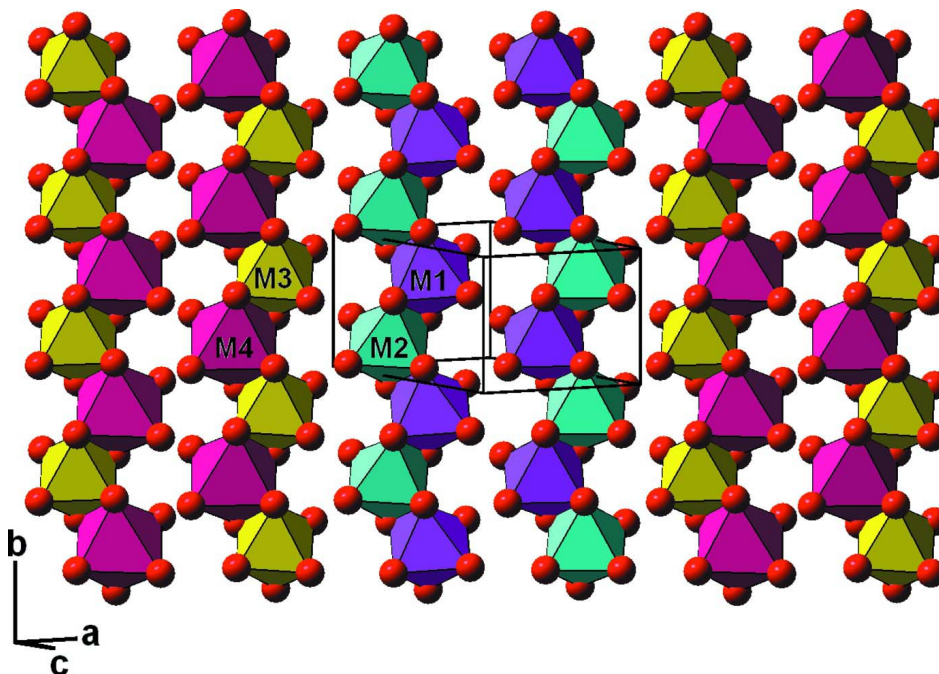
Figure 2

A slice of the lithiotantite structure showing the two types of zigzag edge-shared octahedral chains. All color coding and symbols are as in Figure 1.
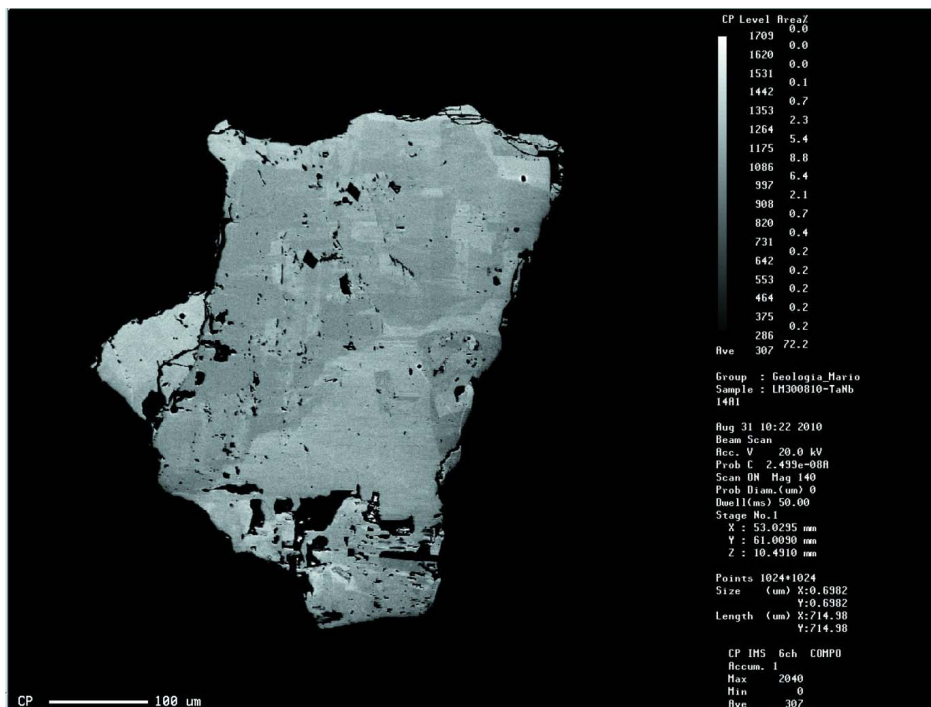
Figure 3

A back scattering electron image of the lithiotantite sample, showing the obvious chemical inhomogeneity of the studied sample. The contrast in darkness reflects the relative distribution of Ta vs. Nb in the sample.

lithium tritantalum octaoxide

Crystal data

$LiTa_3O_8$
$M_r = 607.20$
Monoclinic, $P2_1/c$
Hall symbol: -P 2ybc
$a = 7.4425\ (4)$ Å
$b = 5.0493\ (3)$ Å
$c = 15.2452\ (7)$ Å
$\beta = 107.381\ (3)°$
$V = 546.75\ (5)$ Å^3
$Z = 4$

$F(000) = 1042$
$D_x = 7.377$ Mg m^{-3}
Mo $K\alpha$ radiation, $\lambda = 0.71073$ Å
Cell parameters from 2589 reflections
$\theta = 2.8–32.6°$
$\mu = 45.28$ mm^{-1}
$T = 293$ K
Cuboid, red–brown
$0.06 \times 0.05 \times 0.05$ mm

Data collection

Bruker APEXII CCD area-detector
   diffractometer
Radiation source: fine-focus sealed tube
Graphite monochromator
φ and ω scan
Absorption correction: multi-scan
   (*SADABS*; Sheldrick, 2005)
$T_{min} = 0.172$, $T_{max} = 0.211$

8136 measured reflections
1983 independent reflections
1683 reflections with $I > 2\sigma(I)$
$R_{int} = 0.027$
$\theta_{max} = 32.6°$, $\theta_{min} = 2.8°$
$h = -10 \rightarrow 11$
$k = -7 \rightarrow 7$
$l = -22 \rightarrow 23$

Refinement

Refinement on F^2	Secondary atom site location: difference Fourier map
Least-squares matrix: full	
$R[F^2 > 2\sigma(F^2)] = 0.028$	$w = 1/[\sigma^2(F_o^2) + (0.0077P)^2 + 6.6039P]$
$wR(F^2) = 0.058$	where $P = (F_o^2 + 2F_c^2)/3$
$S = 1.35$	$(\Delta/\sigma)_{max} = 0.002$
1983 reflections	$\Delta\rho_{max} = 2.02$ e Å^{-3}
71 parameters	$\Delta\rho_{min} = -1.92$ e Å^{-3}
1 restraint	Extinction correction: *SHELXL97* (Sheldrick, 2008), Fc*=kFc[1+0.001xFc$^2\lambda^3$/sin(2θ)]$^{-1/4}$
Primary atom site location: structure-invariant direct methods	Extinction coefficient: 0.00065 (6)

Special details

Geometry. All e.s.d.'s (except the e.s.d. in the dihedral angle between two l.s. planes) are estimated using the full covariance matrix. The cell e.s.d.'s are taken into account individually in the estimation of e.s.d.'s in distances, angles and torsion angles; correlations between e.s.d.'s in cell parameters are only used when they are defined by crystal symmetry. An approximate (isotropic) treatment of cell e.s.d.'s is used for estimating e.s.d.'s involving l.s. planes.

Refinement. Refinement of F^2 against ALL reflections. The weighted *R*-factor *wR* and goodness of fit *S* are based on F^2, conventional *R*-factors *R* are based on *F*, with *F* set to zero for negative F^2. The threshold expression of $F^2 > \sigma(F^2)$ is used only for calculating *R*-factors(gt) *etc*. and is not relevant to the choice of reflections for refinement. *R*-factors based on F^2 are statistically about twice as large as those based on *F*, and *R*- factors based on ALL data will be even larger.

Fractional atomic coordinates and isotropic or equivalent isotropic displacement parameters (Å^2)

	x	*y*	*z*	U_{iso}*/U_{eq}	Occ. (<1)
TAM1	0.74765 (4)	0.24400 (7)	0.07791 (2)	0.00508 (9)	0.641 (2)
NBM1	0.74765 (4)	0.24400 (7)	0.07791 (2)	0.00508 (9)	0.359 (2)
TAM2	0.98987 (4)	0.24084 (6)	0.33689 (2)	0.00466 (9)	0.665 (2)
NBM2	0.98987 (4)	0.24084 (6)	0.33689 (2)	0.00466 (9)	0.335 (2)
TAM3	0.50096 (4)	0.23890 (6)	0.333006 (18)	0.00528 (8)	0.874 (2)
NBM3	0.50096 (4)	0.23890 (6)	0.333006 (18)	0.00528 (8)	0.126 (2)
LIM4	0.2391 (10)	0.2561 (17)	0.0794 (5)	0.0030 (13)*	0.96
MNM4	0.2391 (10)	0.2561 (17)	0.0794 (5)	0.0030 (13)*	0.03
NAM4	0.2391 (10)	0.2561 (17)	0.0794 (5)	0.0030 (13)*	0.01
O1	0.0002 (7)	0.0608 (9)	0.0979 (3)	0.0064 (8)*	
O2	0.4176 (7)	0.0670 (9)	0.2181 (3)	0.0059 (8)*	
O3	0.7653 (7)	0.1008 (9)	0.3443 (3)	0.0073 (8)*	
O4	0.5368 (7)	0.4210 (9)	0.1011 (3)	0.0064 (8)*	
O5	0.9144 (7)	0.4112 (9)	0.2154 (3)	0.0054 (8)*	
O6	0.6436 (7)	0.3931 (9)	0.4606 (3)	0.0078 (9)*	
O7	0.8524 (7)	0.5637 (9)	0.0489 (3)	0.0073 (8)*	
O8	0.2755 (7)	0.4123 (9)	0.3444 (3)	0.0063 (8)*	

Atomic displacement parameters (Å^2)

	U^{11}	U^{22}	U^{33}	U^{12}	U^{13}	U^{23}
TAM1	0.00614 (14)	0.00390 (13)	0.00485 (14)	0.00065 (10)	0.00108 (10)	−0.00033 (10)
NBM1	0.00614 (14)	0.00390 (13)	0.00485 (14)	0.00065 (10)	0.00108 (10)	−0.00033 (10)
TAM2	0.00518 (14)	0.00380 (13)	0.00496 (14)	0.00056 (11)	0.00143 (10)	0.00038 (11)
NBM2	0.00518 (14)	0.00380 (13)	0.00496 (14)	0.00056 (11)	0.00143 (10)	0.00038 (11)

TAM3	0.00517 (12)	0.00520 (12)	0.00565 (13)	−0.00042 (10)	0.00190 (9)	−0.00014 (10)
NBM3	0.00517 (12)	0.00520 (12)	0.00565 (13)	−0.00042 (10)	0.00190 (9)	−0.00014 (10)

Geometric parameters (Å, º)

TAM1—O6ⁱ	1.857 (5)	TAM3—O2	1.886 (5)
TAM1—O7	1.901 (5)	TAM3—O8	1.946 (5)
TAM1—O4	1.929 (5)	TAM3—O4ⁱⁱⁱ	1.957 (5)
TAM1—O1ⁱⁱ	2.034 (5)	TAM3—O2^{iv}	2.000 (5)
TAM1—O8ⁱⁱⁱ	2.088 (5)	TAM3—O3	2.045 (5)
TAM1—O5	2.257 (5)	TAM3—O6	2.070 (5)
TAM2—O3	1.849 (5)	LIM4—O7^{vi}	2.079 (9)
TAM2—O1^{iv}	1.887 (5)	LIM4—O3^{iv}	2.099 (10)
TAM2—O5	1.965 (5)	LIM4—O1	2.124 (9)
TAM2—O7^v	1.997 (5)	LIM4—O6ⁱⁱⁱ	2.194 (9)
TAM2—O5^v	2.063 (5)	LIM4—O4	2.296 (9)
TAM2—O8ⁱⁱ	2.266 (5)	LIM4—O2	2.338 (9)
O6ⁱ—TAM1—O7	100.1 (2)	O2—TAM3—O8	103.7 (2)
O6ⁱ—TAM1—O4	102.8 (2)	O2—TAM3—O4ⁱⁱⁱ	92.4 (2)
O7—TAM1—O4	93.5 (2)	O8—TAM3—O4ⁱⁱⁱ	93.6 (2)
O6ⁱ—TAM1—O1ⁱⁱ	94.3 (2)	O2—TAM3—O2^{iv}	94.20 (11)
O7—TAM1—O1ⁱⁱ	89.79 (19)	O8—TAM3—O2^{iv}	91.82 (19)
O4—TAM1—O1ⁱⁱ	161.7 (2)	O4ⁱⁱⁱ—TAM3—O2^{iv}	170.2 (2)
O6ⁱ—TAM1—O8ⁱⁱⁱ	99.5 (2)	O2—TAM3—O3	87.9 (2)
O7—TAM1—O8ⁱⁱⁱ	157.2 (2)	O8—TAM3—O3	168.3 (2)
O4—TAM1—O8ⁱⁱⁱ	93.33 (19)	O4ⁱⁱⁱ—TAM3—O3	87.65 (19)
O1ⁱⁱ—TAM1—O8ⁱⁱⁱ	77.25 (18)	O2^{iv}—TAM3—O3	85.38 (19)
O6ⁱ—TAM1—O5	171.61 (19)	O2—TAM3—O6	168.6 (2)
O7—TAM1—O5	75.44 (18)	O8—TAM3—O6	87.8 (2)
O4—TAM1—O5	84.71 (19)	O4ⁱⁱⁱ—TAM3—O6	86.45 (19)
O1ⁱⁱ—TAM1—O5	78.70 (18)	O2^{iv}—TAM3—O6	85.68 (19)
O8ⁱⁱⁱ—TAM1—O5	83.60 (17)	O3—TAM3—O6	80.72 (19)
O3—TAM2—O1^{iv}	100.9 (2)	O7^{vi}—LIM4—O3^{iv}	95.9 (4)
O3—TAM2—O5	102.5 (2)	O7^{vi}—LIM4—O1	106.0 (4)
O1^{iv}—TAM2—O5	94.4 (2)	O3^{iv}—LIM4—O1	99.2 (4)
O3—TAM2—O7^v	94.7 (2)	O7^{vi}—LIM4—O6ⁱⁱⁱ	98.6 (4)
O1^{iv}—TAM2—O7^v	90.2 (2)	O3^{iv}—LIM4—O6ⁱⁱⁱ	157.0 (4)
O5—TAM2—O7^v	161.0 (2)	O1—LIM4—O6ⁱⁱⁱ	93.9 (4)
O3—TAM2—O5^v	97.94 (19)	O7^{vi}—LIM4—O4	90.4 (3)
O1^{iv}—TAM2—O5^v	158.6 (2)	O3^{iv}—LIM4—O4	78.1 (3)
O5—TAM2—O5^v	91.34 (11)	O1—LIM4—O4	163.5 (4)
O7^v—TAM2—O5^v	78.15 (19)	O6ⁱⁱⁱ—LIM4—O4	84.0 (3)
O3—TAM2—O8ⁱⁱ	173.9 (2)	O7^{vi}—LIM4—O2	165.3 (4)
O1^{iv}—TAM2—O8ⁱⁱ	75.98 (18)	O3^{iv}—LIM4—O2	86.4 (3)
O5—TAM2—O8ⁱⁱ	83.12 (18)	O1—LIM4—O2	87.9 (3)

O7^{v}—TAM2—O8^{ii}	80.15 (19)	O6^{iii}—LIM4—O2	75.2 (3)
O5^{v}—TAM2—O8^{ii}	84.29 (18)	O4—LIM4—O2	75.8 (3)

Symmetry codes: (i) x, $-y+1/2$, $z-1/2$; (ii) $x+1$, y, z; (iii) $-x+1$, $y-1/2$, $-z+1/2$; (iv) $-x+1$, $y+1/2$, $-z+1/2$; (v) $-x+2$, $y-1/2$, $-z+1/2$; (vi) $-x+1$, $-y+1$, $-z$.